Proceedings of the 2007 IEEE
Intelligent Transportation Systems Conference
Seattle, WA, USA, Sept. 30 - Oct. 3, 2007

A Low-cost Vehicle Detection and Classification System based on Unmodulated Continuous-wave Radar

Jianxin Fang, Huadong Meng, Hao Zhang, and Xiqin Wang

Abstract—**Vehicle detection and classification system is an important part of the Intelligent Transportation systems (ITS). Its function is to measure traffic parameters such as flow-rate, speed, and vehicle types, which are valuable information for applications of road surveillance, traffic signal control, road planning, and so on. This paper presents a novel low-cost vehicle detection and classification system which is based on a K-band unmodulated CW radar. This system utilizes time-frequency analysis, multi-threshold detection, and Hough Transform as the major signal processing methods to extract speed and shape information of vehicles from Doppler signature they generate. It can perform vehicle detection, speed measurement, and vehicle classification simultaneously. Experimental results show that the proposed system and algorithms can provide promising performance and accuracy.**

I. Introduction

Vehicle detection and classification system is an important part of Intelligent Transportation Systems (ITS). Its function is to measure traffic parameters such as speed, flow-rate, and vehicle types, which are useful information for applications of road surveillance, traffic signal control, road planning, and so on [1]-[3]. Current vehicle detection and classification systems are mainly based on ultrasonic sensors, acoustic sensors, infrared sensors, inductive loops [4], magnetic sensors [5], video sensors [6], laser sensors [7], and microwave radars [8] [9]. However, ultrasonic, acoustic, and infrared sensors lack of stability in noisy environments; the inductive loops and magnetic sensors involve disruptive installation process and are liable to damages [10]; the video and laser sensors are usually vulnerable to weather and light conditions, not suitable for all-weather working. In comparison, microwave radar systems have high speed-measurement accuracy, and are easier for installation, more robust and less vulnerable to weather, thus tend to be more promising in both research and application.

The microwave radars for traffic applications mostly work on X-band (around 10 GHz) or K-band (around 24 GHz), with fixed antennae. According to the system type, they can usually be divided into pulse Doppler (PD) radars, unmodulated CW radars, and frequency-modulated CW (FMCW) radars. RTMS [11] is an example of existent systems, which is based on FMCW radar and provides capabilities of measuring parameters such as traffic volume, vehicle presence, lane occupancy, vehicle speed, queue length, etc.

Radar-based vehicle detection and speed measurement techniques mostly mature and are widely used, but in comparison the development of vehicle classification remains premature in laboratory. There are three major kinds of target classification techniques using microwave radars: Doppler signature, height profile, and combination of distance and Doppler. Techniques based on Doppler signatures [12]-[15] are used to divide targets into several macro groups such as aircrafts, vehicles, creatures, and so on, but have not been used specifically for vehicle classification. Techniques based on height profiles [8], [9] and on the combination of distance and Doppler information [16] require complicated high-resolution radar devices, which are usually expensive, and thus limit their applications.

On the other hand, the simple-structured low-cost CW radars can provide Doppler information for vehicle detection and speed measurement, but are rarely applied to classification because only the speed information can be easily drawn and used. In this paper, a novel vehicle detection and classification system using unmodulated CW radar is presented. The classification algorithm of this system utilizes Doppler signature to estimate the spatial distribution of scattering centers of target vehicles so to discriminate vehicles with different distributions. With this new approach, one single CW radar can perform vehicle detection, speed measurement, and vehicle classification simultaneously.

The rest part of this paper is organized as follows. Section II introduces the structure and implementation of the system. Section III discusses the working principle of the system, including the scenario, radar signal, and signal processing approaches for detection and classification. Section III gives test results of the proposed system and algorithms as a performance evaluation. Conclusions are given in the last section.

II. System Implementation

A. System Structure

The vehicle detection and classification system consists of four major parts: the antenna, the microwave radio front, the analog signal amplifier and the digital signal processor (DSP). The prototype system also includes a data acquisition and

Manuscript received April 2, 2007. This work was supported in part by the National Natural Science Foundation of China (NSFC) under Grant XXXXXX.

Jianxin Fang, Huadong Meng, Hao Zhang, and Xiqin Wang are with the Department of Electronic Engineering, Tsinghua University, Beijing 100084 China. (Corresponding author is Xiqin Wang. Phone: +8610-62781378-16; fax: +8610-62773837; e-mail: wangxq_ee@ tsinghua.edu.cn).

feed interface for research and development. The block diagram of this system is shown in Fig. 1.

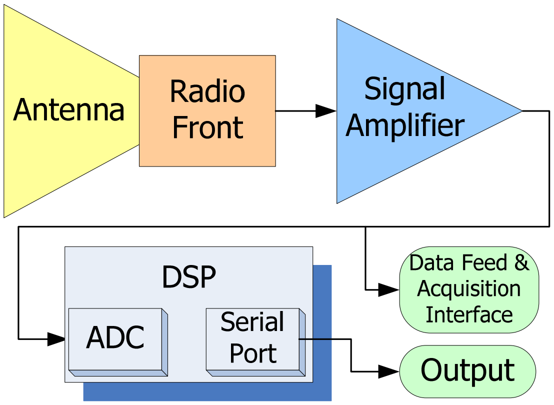

Fig. 1. Block diagram of the vehicle detection and classification system.

In this system, the microwave radio front is implemented with a Gunn Transceiver working at K-band. The receiver is in zero-intermediate frequency (ZIF) structure and directly outputs Doppler signals. The radar uses a horn antenna, whose main beam points at a long narrow area that approximately matches a lane of the road. The radar should be mounted above the lane on which vehicles run through the radar illuminated zone facing the radar antenna. The analog signal amplifier is implemented with two stages of operation amplifiers (OPAMP). The parameters of the radar system are listed in Table I.

TABLE I
PARAMETERS OF THE RADAR SYSTEM

Description	Symbol	Value	Unit
Suggested height of mounting	h_0	7-9	Meter
Suggested elevation angle of antenna	α	45	Degree
Type of the radar	Unmodulated continuous wave		
Carrier Frequency	f	24.125	GHz
Output Power	P_t	5	mW
Receiver Sensitivity	S	-90	dBc
Type of the radar antenna	Horn antenna		
Elevational plane beamwidth	γ	30	Degree
Horizontal plane beamwidth	β	20	Degree
Gain of the antenna	G_{ant}	17	dB
Gain of the analog amplifier	G_{amp}	60	dB
Bandwidth of the analog amplifier	B_{amp}	10	kHz
Sampling frequency of ADC	f_s	20	kHz

The DSP part is implemented with *TMS320F2808* by *Texas Instruments*. It features a high-performance 100-MIPS 32-bit CPU, integrated A-D converters, Flash memories, and serial communication ports. This DSP has sufficient processing ability and can be applied with very few extra components, which is helpful for the simple structure and low cost of the entire system. Currently, a prototype system has been finished, with a small dimension of 4 cm × 5 cm × 16 cm, as shown in Fig. 2. The total cost of this system is lower than \$200 USD. The simple structure, small size, and low cost make this system competitive against the existent products.

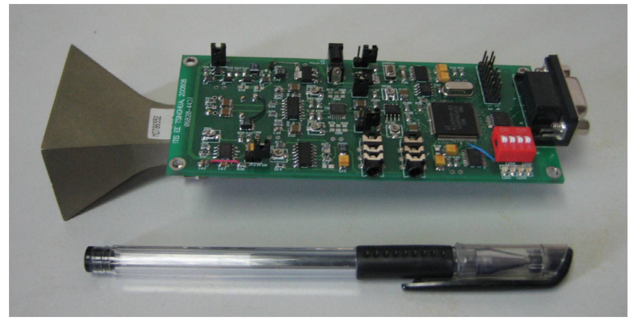

Fig. 2. Photograph of the current prototype system.

B. *Software Framework*

The signal processing software of the microwave vehicle detection and classification system is implemented in the DSP, mainly consisting of four modules: the pre-processing module, the detection algorithm, the classification algorithm and the interface and control module. The framework of the signal processing software is shown in Fig. 3.

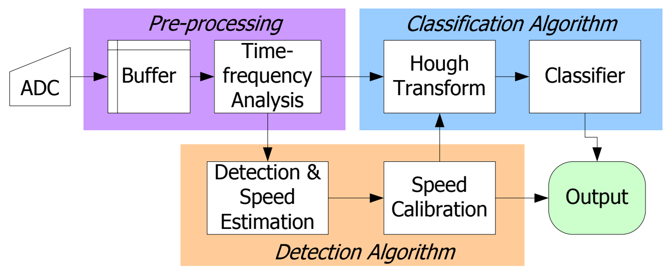

Fig. 3. Framework of the signal processing software.

The detailed working principle of the system, the detection algorithm and the classification algorithm are introduced in the following section.

III. PRINCIPLES OF WORKING

A. *Working Scenario and Radar Signal*

The basic working scenario of this vehicle detection and classification system is shown below in Fig. 4. In this scenario, the radar is mounted at the height h_0 from the ground. The radar antenna faces the ground with elevation angle α and elevation beamwidth γ. A coordinate system $x-h$ is set up for this scenario. The radar illuminated zone along x-axis, $[x_1, x_0]$, can be written as

$$\begin{aligned} x_0 &= \frac{h_0}{\tan(\alpha-\gamma/2)} \\ x_1 &= \frac{h_0}{\tan(\alpha+\gamma/2)} \end{aligned}. \tag{1}$$

This system is designed to detect the approaching vehicles, which run in the $-\vec{x}$ direction. For instance, a running passenger car with speed v is shown in Fig. 4.

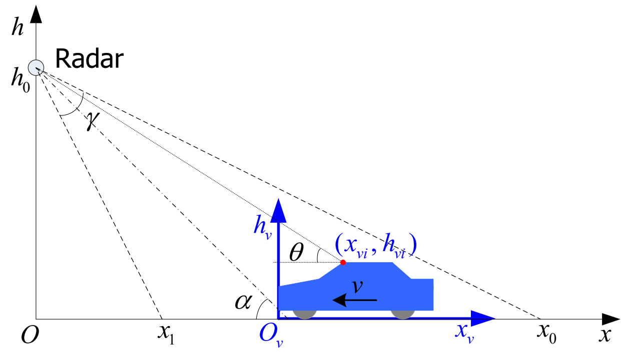

Fig. 4. Working scenario of the system.

Considering the actual scales of the scenario in Fig. 4, vehicles should be considered as body targets composed of multiple scattering centers. In order to analyze the corresponding Doppler signals, a vehicle coordinate system $x_v - h_v$ is also introduced as shown in Fig. 4, with its origin O_v determined by the position of vehicle head.

For convenience of analysis, the scattering centers of the target vehicle are denoted as $(x_{vi}, h_{vi}), i = 1,...,n$. Assume that the vehicle runs through the radar illuminated zone at a constant speed *v*, and set $t = t_0$ (referred as *entering time*) when O_v reaches the start position x_0 of the zone, coordinates of these key points can be transformed to the $x - h$ system as

$$\begin{aligned} x_i &= x_0 + x_{vi} - v(t - t_0) \\ h_i &= h_{vi} \end{aligned} . \tag{2}$$

Then the frequency of Doppler signal produced by each scattering center can be expressed as

$$\begin{aligned} f_{di}(t) &= \frac{2vf}{c} \cos\theta_i(t) \\ &= \frac{2vf}{c} \frac{x_0 + x_{vi} - v(t - t_0)}{\sqrt{(x_0 + x_{vi} - v(t - t_0))^2 + (h_0 - h_{vi})^2}} \end{aligned} \tag{3}$$

in which *f* is the radio frequency of the radar and *c* is the speed of light.

Equation (3) shows that the Doppler frequency as a function of time *t* is also determined by speed *v* and the spatial distribution of scattering centers in the vehicle coordinate system, $(x_{vi}, h_{vi}), i = 1,...,n$. In order to analyze the Doppler frequency intuitively, several empirical scattering centers are assumed on the corners and edges of the vehicle surface in Fig. 5-A, and corresponding simulation results of the Doppler frequency varying with time is shown in Fig. 5-B.

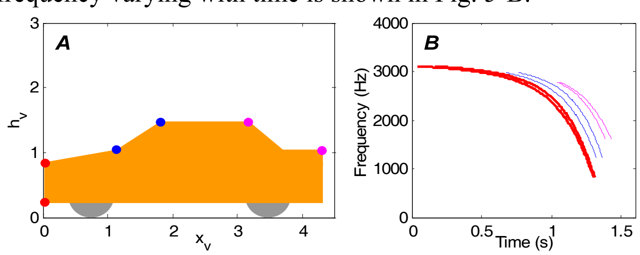

Fig. 5. Empirical scattering centers and corresponding Doppler frequency

Fig. 5 implies that the reflected signal from a vehicle in this scenario exhibits a special *Doppler signature* composed of a cluster of non-intersected curves on the time-Doppler ($t - f_d$) plane, with each curve generated by one scattering center. This special Doppler signature is formed because the elevation angle θ_i of each scattering center is increasing as the vehicle is moving, generating a decreasing Doppler frequency, and different scattering centers generate curves with different positions on the $t - f_d$ plane.

For real Doppler signal generated by target vehicles, in order to obtain the time-varying frequency components, joint time-frequency analysis is utilized to process the digitized radar signal. Here short-time Fourier transform (STFT) is used to carry out the time-frequency analysis. A segment of the radar signal, its spectrogram (the result of STFT) and the corresponding vehicle photo is shown in Fig. 6.

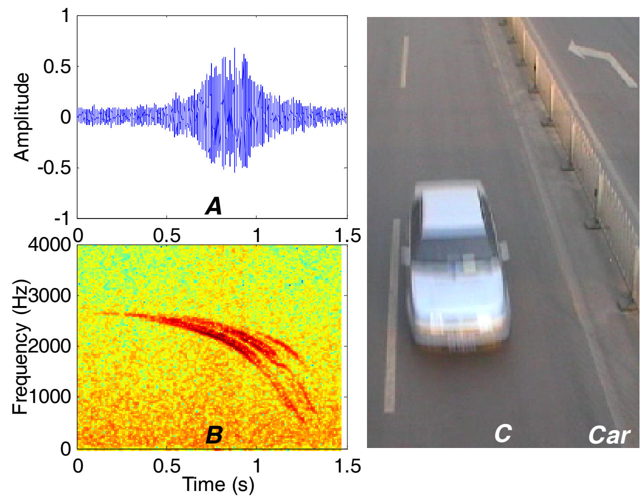

Fig. 6. The radar signal, Doppler signature, and the photo of target vehicle.

In Fig. 6-B, the real Doppler signature of running vehicle matches the simulation result quite well. Further analysis shows that vehicles of different shapes generate Doppler signatures of different styles. So it is proved that the Doppler Signature carries information about the speed and shape of target vehicle and thus can be used for detection and classification.

B. Detection Algorithm

For this system, the frequency of received signal is directly related to the carrier frequency and the speed of the target, whereas the spectrum of noise follows certain distribution and is usually stationary versus time. Therefore, detection and speed estimation of target vehicles can be implemented simultaneously by threshold detection over the STFT results. According to the special characteristics of the Doppler signature, a multi-threshold detection algorithm is designed to seek for better performance of both detection and classification algorithms. For each target, the detection procedure is as follows. A demonstration is given in Fig. 7.

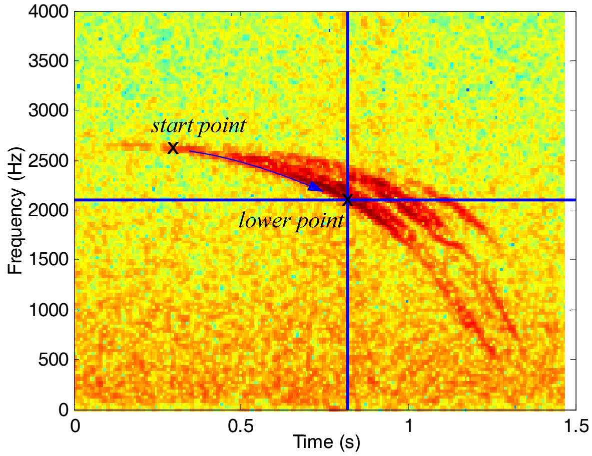

Fig. 7. The multi-threshold detection algorithm with ρ=0.8.

Step 1, *start point* detection. A power threshold TH_1 is set on the STFT result to search for the start point of the Doppler signature, as shown in Fig. 7. TH_1 is relatively low in order to increase sensitivity so that potential target can be detected as early as possible, with preferable speed estimation accuracy. Note that in the beginning part of the Doppler signature, Doppler frequency decreases very slowly with time, so an early detection is helpful for maintaining a high accuracy of speed estimation. Given the coordinates of the start point, $(t_{start}, f_{d.start})$, the estimate of target speed and entering time can be obtained with

$$\hat{v} = \frac{cf_{d.start}}{2f\cos(\alpha-\gamma/2)}. \qquad (4)$$
$$\tilde{t}_0 = t_{start}$$

Step 2, frequency tracking and *lower point* detection. After Step 1, a frequency threshold TH_2= $\rho f_{d.start}$ is set on the STFT result with the typical value $\rho = 0.7$ to 0.9. The lowest frequency component of the Doppler signature is tracked until it reaches TH_2 and triggers the detector. The detection point on the Doppler signature is called the *lower point*. Assume the target vehicle runs at a constant speed, we can get an estimate of entering time with better precision from the coordinates of the lower point, $(t_l, \rho f_{d.start})$,

$$\hat{t}_0 = t_l - h\left(\frac{1}{\tan(\alpha-\gamma/2)} - \frac{\rho\cos(\alpha-\gamma/2)}{\sqrt{1-\rho^2\cos^2(\alpha-\gamma/2)}}\right)/\hat{v}. \qquad (5)$$

Step 3, signal power verification. Once the lower point is got, a power threshold TH_3 is set for the Doppler signal. If the total signal power at t_l exceeds TH_3, the potential target is confirmed with speed $\hat{v}$ and entering time $\hat{t}_0$, and the detection procedure is finished; otherwise the target is discarded and the detection procedure is aborted. TH_3 is selected according to the signal power of actual target vehicles; it is usually much higher than TH_1 in order to provide a target verification mechanism.

This multi-threshold detection algorithm has several advantages over single-threshold detection. First, it has better capability of resisting noise and jamming, which helps reduce the false alarm rate remarkably. Second, the detection of lower point can improve the estimation accuracy of t_0, which is important for the following classification algorithm. Third, the verification stage can effectively reduce false alarms caused by the vehicles from other lanes.

C. *Classification Algorithm*

According to the analysis above, Doppler signature carries information about the spatial distribution of scattering centers, which is determined by the geometry and material characteristics of target vehicle. Therefore if we can extract the spatial distribution of scattering centers from Doppler signature, the shape of the target vehicle can be inferred and the type can be discriminated. This is the basic principle of the classification algorithm of the proposed system. Hough Transform is utilized to accomplish this task.

Hough Transform is a mapping methodology between image space and parameter space. It is widely used in image processing problems to detect curves with known shapes, such as straight lines, circles, and any other curves that can be described by parameter equations. By Hough Transform, a curve *C* in the image space is mapped to a cluster of curves intersecting at one point in the parameter space. And the coordinates of this point equal to the parameter values of curve *C*. So curves in the image space can be detected and their parameters can be estimated by searching for the intersection points in the parameter space.

In this system, Hough Transform is used to estimate the positions of scattering centers, denoted by $(x_{vi}, h_{vi}), i = 1,...,n$, from the Doppler signature. Consider the $t-f_d$ plane and the $x_v - h_v$ plane as the image space and the parameter space respectively, then each component $f_{di}(t)$ of the Doppler signature is a curve of known shape, described by (3) with parameters (x_{vi}, h_{vi}). These parameters represent the positions of the scattering centers and will be extracted from the Doppler signature by Hough Transform. In order to implement the Hough Transform, Equation (3) can be transformed to express h_v as a function of x_v with t and f_{di} as parameters:

$$\begin{aligned} h_v(x_v) &= h_0 - (x_v + x_0 - v(t-t_0))\sqrt{\left(\frac{2vf}{f_{di}(t)c}\right)^2 - 1} \\ &= h_0 - (x_v + x_0 - v(t-t_0))\tan\theta_i(t) \end{aligned}. \qquad (6)$$

Equation (6) shows that each point $(t, f_{di}(t))$ on the *i*th curve of the Doppler signature is mapped to a straight line in the $x_v - h_v$ space. The slope of the line $h_v(x_v)$ is $-\tan\theta_i$, where $\theta_i(t)$ represents the elevation angle of the *i*th scattering center at time t with respect to the radar. Furthermore, all the lines $h_v(x_v)$ mapped from points (t, f_{di})'s on the same curve of the Doppler signature should intersect at the same point (x_{vi}, h_{vi}) in the $x_v - h_v$ plane.

Clusters of lines mapped from other curves of the Doppler signature should intersect at their corresponding points, as demonstrated in Fig. 8. Theoretically, all these intersection points actually are the scattering centers. Therefore, Hough Transform figures out the spatial distribution of scattering centers in the vehicle coordinate system from the Doppler signature, and decouples this distribution from speed and position.

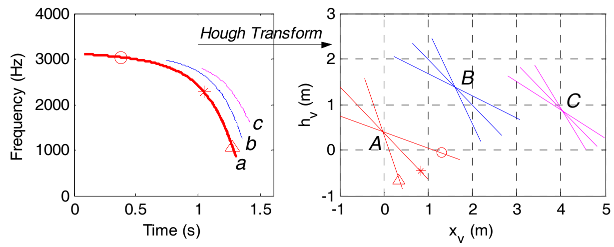

Fig. 8. The demo process of Hough Transform.

Fig. 9 gives the real Doppler signature and Hough Transform results of five typical vehicles.

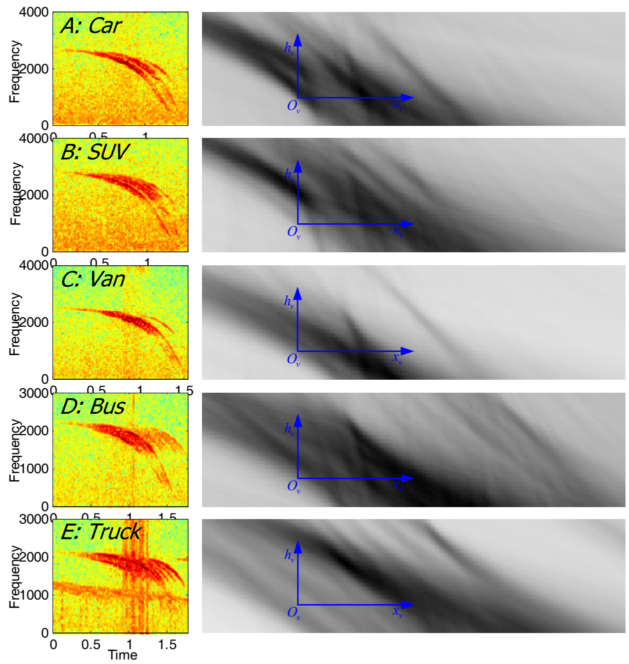

Fig. 9. Doppler signature and Hough Transform of five typical vehicles.

In the results of Hough Transform, each cluster of lines does not perfectly intersect at one point as the theoretical result. Instead, intersection points degrade into blurred stripes and areas. However, the distribution of the darkness in the transform result can roughly exhibit the real distribution of scattering centers, thus can be used for classification.

Based on the Hough Transform results, a simple classifier is designed to divide vehicles into three classes: (A) small-size vehicles including cars and SUVs, (B) middle-size vehicles including vans, (C) large-size vehicles including buses and trucks.

In order to extract significant features, the result of Hough Transform is first distorted by 45 degrees to turn the stripes vertical. Then the maximum value of each column is picked out to form a new vector. Finally, by using Principle Component Analysis (PCA), these vectors are compressed to a lower dimension for the classifier. The process of feature extraction and examples of each class are shown in Fig. 10.

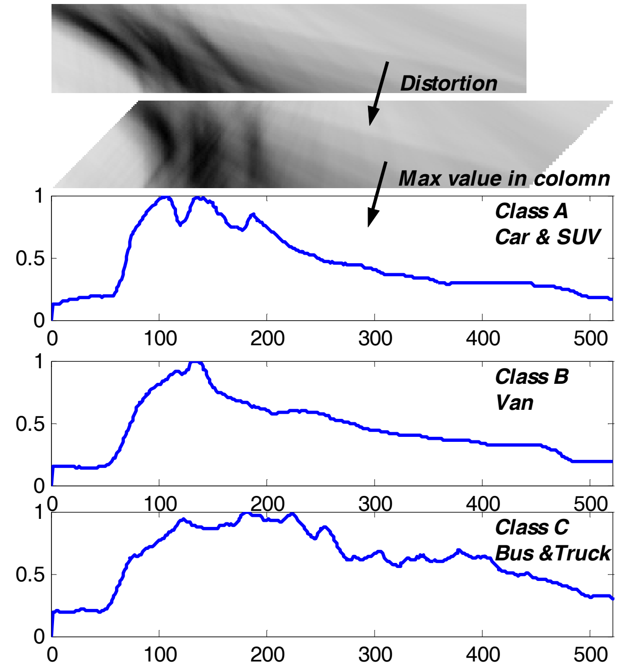

Fig. 10. The process of feature extraction.

The classifier is composed of three linear sub-classifiers to divide samples into classes A-B, A-C and B-C separately. The final result is generated from the sub-results on a voting basis: if a sample is put in the same class X (either A, B, or C) by any two of the three sub-classifiers, the final classification result will be X; if three sub-classifiers give three different results, the sample's distances to the classification boundaries in the sub-classifiers are considered, and the class with maximum distance is elected as the result.

IV. Test Results

Experiments were conducted in the urban area of Beijing, China. The basic scenario of the experiments is the same as shown in Fig. 4. Radar signal was recorded and imported into computer for further analysis. Both the radar and the data acquisition equipment were installed on pedestrian overpass. A video camera was installed nearby to record vehicles passing the radar's view for further verification of the radar data. Following performance evaluation is based on the results of field experiments and analysis of the acquired data.

A. Detection Algorithm

The proposed multi-threshold detection algorithm works well in the system. The comprehensive testing of this detect algorithm is still in progress. Current result shows that, the false alarm rate caused by noise and jamming is extremely low. The false alarms caused by vehicles from other lanes are mostly eliminated by the algorithm. The detection rate in expedite traffic conditions is above 95%. The accuracy of speed estimation is also promising. A data set of calibrated speed measurement compared with actual vehicle speed is given in Table II. The actual vehicle speed is recorded with a special device installed on the experiment vehicle.

TABLE II
TESTING RESULT OF SPEED ESTIMATION

Vehicle Number	Actual Speed (km/h)	Calibrated Speed Measurement (km/h)
1	88	89
2	123	127
3	116	118
4	104	109
5	60	58
Average Accuracy of Speed Measurement:	97.1%	

B. Classification Algorithm

After time-frequency analysis and detection, 164 vehicle samples are picked out from the experiment data. Most vehicles in the sample set are cars and SUVs; others are vans, buses and trucks. The diversity of these vehicle samples is not so significant to cover all vehicle types, but it is enough to demonstrate the effectiveness of the proposed classification algorithm.

Samples were divided into a training set and a testing set randomly for 20 times. Each time, the training set was used to train the classifier, and the testing set was used to examine the classification accuracy. Results are averaged over the 20 times of testing, and a total average accuracy of 94.8% is achieved. The detailed average results of classification are given below in Table III.

TABLE III
THE FINAL CLASSIFICATION RESULT (AVERAGE OF 20 TIME CALCULATION)

Observed	Total Number	Classified A			Accuracy
		Class A	Class B	Class C	
Class A Car & SUV	135	**128.95**	4.53	1.52	**95.5%**
Class B Van	17	1.35	**15.56**	0.09	**91.5%**
Class C Bus & Truck	12	0.70	0.31	**10.99**	**91.6%**
Total	**164**	**-**	**-**	**-**	**94.8%**

The experiment and test results for detection and classification algorithms prove that both of the proposed algorithms are effective and accurate for the current applications. It is also proved that the proposed system performs well in the testing environment. In the future, research and experiment will be continued in order to improve the algorithms as well as the entire vehicle detection and classification system so that the system can better meet the requirements of practical applications.

V. CONCLUSION

In this paper, a novel vehicle detection and classification system based on unmodulated CW radar is presented. This system uses K-band Gunn transceiver as radio front and DSP chip as signal processing unit. It is much less expensive than other kinds of traffic sensors. STFT is used in the pre-processing stage to obtain Doppler signature of the target. A multi-threshold algorithm is designed to achieve better and robust detection performance. Hough Transform is utilized to extract the spatial distribution of target's scattering centers, based on which the classification is realized. Test results prove that the proposed algorithms are effective and accurate; the detection and classification system is reliable under the testing conditions. In the future, research and experiment will be continued. The detection algorithm will be further tested and tuned. The class model will be extended for more vehicle types. The entire system will be improved and tested to better meet the requirements of practical applications.

REFERENCES

[1] D. Chen, X. Gong, C. Zheng. "A wireless traffic information collection system in Beijing urban freeways," in *2002 Proc. IEEE 5th Int. Conf. Intelligent Transportation Systems*, pp. 387-391.

[2] Y. S. Yang. "A case study of highway traffic flow model - model validation and simulation," in *2002 Proc. Int. Conf. Control Applications*, Vol 2, pp. 978-983.

[3] F. N. McLeod, N. B. Hounsell, and B. Rajbhandari, "Improving traffic signal control for pedestrians," in *2004 IEE 12th Int. Conf. Road Transport Information and Control*, pp. 268-277.

[4] J. Gajda, R. Sroka, M. Stencel, A. Wajda, and T. Zeglen, "A vehicle classification based on inductive loop detectors," in *2001 Proc. 18th IEEE Conf. IMTC*, vol. 1, pp. 460-464.

[5] S. Cheung, *et al*. "Traffic measurement and vehicle classification with single magnetic sensor," in *Journal of the Transportation Research Board, No. 1917*, TRB, National Research Council, Washington, D.C., 2005, pp. 173-181.

[6] S. Gupte, O. Masoud, R. F. K. Martin, and N. P. Papanikolopoulos, "Detection and classification of vehicles," in *IEEE Trans. Intelligent Transportation Systems*, vol. 3, No. 1, Mar. 2002, pp. 37-47

[7] H. M. Abdelbaki, K. Hussain, and E. Gelenbe, "A laser intensity image based automatic vehicle classification system," in *2001 Proc. IEEE Conf. Intelligent Transportation Systems*, pp. 460-465.

[8] I. Urazghildiiev, et al, "A vehicle classification system based on microwave radar measurement of height profiles," in *2002 Proc. Int. Conf. RADAR*, pp 409-413.

[9] Y. Xuan, H. Meng, X. Wang, and H. Zhang, "A high-range-resolution microwave radar system for traffic flow rate measurement," in *2005 Proc. IEEE Conf. Intelligent Transportation Systems*, pp. 880-885.

[10] K. W. Dickinson, C. L. Wan, "An evaluation of microwave vehicle detection at traffic signal controlled intersections," in *1990 Int. Conf. Road Traffic Control*, pp. 153-157.

[11] J. Wang, E. R. Case, D. Manor, "The road traffic microwave sensor (RTMS)," in *1992 Int. Conf. Vehicle Navigation and Information System*, pp. 83-90.

[12] J. J. Martinez Madrid, J. R. Casar Corredera, and G. de Miguel Vela, "A neural network approach to Doppler-based target classification," in *1992 Proc. Int. Conf. Radar*, pp. 450-453.

[13] M. Jahangir, K. M. Ponting, and J. W. O'Loghlen, "A robust Doppler classification technique based on Hidden Markov Models," in *2002 Proc. Int. Conf. RADAR*, pp 162-166.

[14] J. Kjellgren, S. Gadd, N. Jonsson, and J. Gustavsson, "Analysis of Doppler measurements of ground vehicles," in 2005 *Proc. IEEE Int. Conf. Radar*, pp 284-289.

[15] I. Bilik, J. Tabrikian, and A. Cohen, "Target classification using Gaussian mixture model for ground surveillance Doppler radar," in *2005 Proc. IEEE Int. Conf. Radar*, pp 910-915.

[16] H. Roe and G. S. Hobson, "Improved discrimination of microwave vehicle profiles," in *1992 IEEE MTT-S Int. Microwave Symposium Digest*, vol. 2, pp 717-720.